Effect of the Particle Size and Particle Agglomeration on Composite Membrane Performance

M. G. García, J. Marchese, N. A. Ochoa

Instituto de Física Aplicada (INFAP), Consejo Nacional de Investigaciones Científicas y Técnicas (CONICET), Fondo para la Investigación Científica y Tecnológica (FONCYT), Universidad Nacional de San Luis (UNSL), Chacabuco 917-5700, San Luis, Argentina

Received 14 December 2009; accepted 11 February 2010
DOI 10.1002/app.32274
Published online 22 June 2010 in Wiley InterScience (www.interscience.wiley.com).

ABSTRACT: One of the most used methods for studying the rigidification of polymer matrices in composite membranes is differential scanning calorimetry. Glass-transition temperatures give information about filler–polymer interaction and the rigidity of the polymer matrix. In this study, optical microscopy, mechanical property testing, and X-ray diffraction, instead of differential scanning calorimetry, were used to study both poly(ether imide) (PEI) matrix rigidification and activated carbon–PEI interfacial adhesion. Then, the permselective properties of the mixed matrix membranes were interpreted. The change in rigidity in these composite membranes was in agreement with the decrease in the flexibility of the composite materials as the filler content increased. This fact was confirmed by the tension and elongation data and X-ray diffraction (DRX) measurements. However, the Young's modulus value decreased as the carbon content increased. There was an increase in all of the gas permeability coefficients measured in the composites compared with that of PEI. As the particle size grew, a low particle surface area and a poor interfacial adhesion were observed. The carbon agglomerates acted as sites of stress concentration within the polymeric matrix. This decreased the intercatenary distances and limited the movement of polymer chains, which resulted in a more rigid matrix. The higher selectivity of the H_2/CH_4, H_2/CO_2 and O_2/N_2 systems observed in the composite membranes revealed that there were both a preferential sorption of certain gases in the carbon surface or carbon–polymer interface and a molecular size exclusion, which were responsible for that increment, despite the poor interfacial adhesion. J Appl Polym Sci 118: 2417–2424, 2010

Key words: barrier; composites; gas permeation; membranes

INTRODUCTION

Nowadays, the main challenge in membrane technology is to improve existing membrane processes and to extend their applications. Many studies have been devoted to the investigation of different membrane materials and the development of new membrane structures exhibiting a high selectivity and intrinsic permeability to specific gases.[1–4]

In the past 2 decades, in particular, two new types of materials have been extensively studied in terms of their high performance in the presence of aggressive agents: crosslinked polymers and mixed matrix materials. Crosslinking techniques are used as an effective tool to stabilize the properties of polymeric membranes for gas permeation. These techniques may apply chemical or physical methods.[5] Kita et al.[6] and Liu et al.[7] investigated the effect of UV crosslinking on the performance of gas transport. Bos et al.[8] and Krol et al.[9] induced reactions of Matrimid crosslinking above 200°C and studied their effects on the separation of gases and hydrocarbons. Wind and coworkers[10,11] crosslinked polyimides containing carboxylic acid side groups with ethylene glycol and aluminum acethylacetonate at high temperatures and suggested covalent crosslinking as a possible mechanism of the reaction.[12]

Furthermore, mixed matrix composite films composed of two different materials offer the potential of combining polymer processability with the gas-separation properties of rigid molecular sieve materials. It has lately been determined that composites based on polymers reinforced with a small amount of inorganic filler can significantly improve the mechanical, thermal, and barrier properties of pure polymeric matrices.[13] The successful implementation of these materials depends on the polymeric matrix selection, the inorganic filler, and the elimination of polymer–filler interfacial defects. It has generally been observed that when rubber is used as a polymeric matrix, there is adequate contact between the disperse and organic phases. However, polymeric rubber matrices with high gas fluxes present low selectivity. In the case of glassy polymers, the contact between the polymeric phase and the inorganic particles is diminished because of weak polymer–filler interactions, which tend toward the formation of voids in the interface of materials.[14,15] To improve the interfacial contact, several techniques have been

Correspondence to: N. A. Ochoa (aochoa@unsl.edu.ar).

used. For example, in their preparation of zeolite-filled glassy polymer membranes, Duval et al.[16] found poor adhesion between the polymer phase and the external surface of the particles. To tackle this problem, various methods have been investigated, such as modification of the external surface of zeolite particles, preparation of the composite material at the temperature of the polymer's glassy transition, and thermal treatment. Kumar et al.[17] studied the mechanical, morphological, and electrical properties of poly(ether imide)-carbon nanofiber composite. They purified the carbon nanofibers, ball-milled and functionalized them, and treated their surfaces with plasma to decrease particle agglomeration and the generation of interfacial defects. The procedure of functionalization consisted of the treatment of the carbon nanofibers with a mixture of concentrated acids (H_2SO_4–HNO_3) at 90°C for 10 min to induce the formation of carboxylic groups on the nanotube surface and to generate chemical bonds with the polymeric matrix's functional groups to ensure a good dispersion and interfacial contact between them. Vu et al.[18] prepared mixed matrix membranes by using carbon molecular sieve (CMS) particles as the selective inorganic filler. The CMS particles were incorporated into two commercial glassy polymeric matrices: Ultem 1000 (PEI) and Matrimid 5218 (polyimide); these exhibited excellent polymer–filler contact and a high selectivity to CO_2/CH_4 with respect to the pure polymers.

In a previous article,[14] we reported an alternative preparation of poly(acrylonitrile-butadiene-styrene) (ABS)-based membranes for CO_2/CH_4 separation with inorganic filler materials, which differed substantially from the molecular sieves normally used. In another study,[19] we analyzed the structure of carbon aggregates, the distribution of smaller carbon particles inside the polymeric matrix (using ABS copolymer), and the subsequent modifications in the membrane morphology for different volume fractions of two activated carbons (ACs), along with the resulting permeabilities and selectivities (CO_2/CH_4, O_2/N_2).

In this study, the selected filler material was a microporous AC, and the polymer used was an amorphous, thermoplastic PEI with excellent mechanical, permselective, and thermal properties due to its high glassy temperature.[17,20] The influence of AC content on the structural changes in the polymeric phase was studied in relation to both the mechanical and permselective properties of this composite material.

EXPERIMENTAL

Materials

Pellet like PEI (Ultem 1000, General Electric, Pittsfield, MA) was used as the continuous phase of the mixed matrix membranes. This polymer was synthesized from the following monomers: dianhydride 2,2′-bis[4-(3,4-dicarboxyphenoxy) phenyl]propane (BPADA), and 1,3-phenylendiamine. It had a glass-transition temperature around 209°C and a density of 1.27 g/cm^3 at 25°C.[19] Dichloromethane (Fluka, Sigma-Aldrich, Bs.As, Argentina) was used as a solvent. Figure 1 illustrates the repetitive unit of polymer.

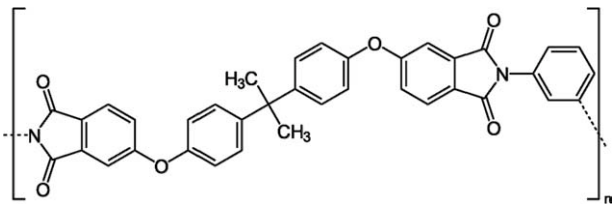

Figure 1 PEI unit structure.

The AC Maxsorb 3000, a powder with a high surface area provided by Kansai Coke & Chemical Co., Ltd. (Kakogawa, Japan), was used as an inorganic dispersed phase in the polymeric matrix. Marchese et al.[14] reported the structural characteristics of the AC, namely, the surface area (3272 m^2/g), pore size distribution (between 7 and 30 Å), mean pore width size (21.7 Å), high porosity ($\varepsilon = 0.87$), and particle size distribution (between 0.2 and 20 μm).

The pure gases used for this study included hydrogen, nitrogen, oxygen, methane, and carbon dioxide because they provided information about several industrially pertinent separations. The purity of the pure gases was more than 99.95%, and they were supplied by Air Liquid (Córdoba, Argentina).

Preparation of the mixed matrix films

First, a PEI polymer solution was prepared by the dissolution of 7% (w/v) PEI in the Cl_2CH_2 solvent with continuous stirring with a magnetic bar at 300 rpm for 4 h at 298 K. The Erlenmeyer glass containing the PEI solution was placed in an ultrasonic bath. Then, the corresponding amount of AC (0–20% w/w) was gently added to the PEI solution under mechanical stirring and sonication at ambient temperature (298 K) for 1 h. Sonication and stirring enhanced the homogeneous distribution of the carbon particles in the polymer solution and decreased the formation of carbon agglomerates. The obtained suspensions were cast (previous filtering) at 25°C in air (relative humidity = 45%) with a film extensor onto a glass plate. The resulting films were dried *in vacuo* at 80°C for 48 h. Thus, the resulting thickness ranged from 75 to 125 μm and was measured with a Köfer micrometer (Germany) (precision = ±1 μm).

Composite material characterization

Optical microscopy (OM)

The topography of the prepared membranes was studied by OM. Images were obtained on an NanoScope OMV-PAL optic system (USA), which took images in a digital format. They were analyzed with the ScanPro image program (USA) to obtain information on the particle agglomeration as the AC content increased.

Mechanical properties

The mechanical properties were measured with a Comten Industries Series 94 VC instrument (USA) at a constant traction speed of 5 mm/min.

To ensure complete relaxation of the polymeric structures and to standardize the experimental procedure, the mechanical properties were measured at room temperature ($T = 25°C$) and at a relative humidity of 40% 24 h after the film casting. The results are the average values from three samples of each membrane.

Wide-angle X-ray diffraction (WAXD)

WAXD studies were carried out with a Rigaku model D-Max III C (USA) with a Cu Kα lamp and a nickel filter. The diffractograms obtained for the mixed matrix membranes correspond to completely amorphous materials, as expected for polymers, and AC presented broad bands in a range of 2θ between 5 and 60°. From the diffractograms, the *d*-spacings of each synthesized composite material were determined by Bragg's equation:

$$n\lambda = 2d \sin \theta \tag{1}$$

where n is the integer determined, λ is the wavelength of the X-ray (nm), and θ is the time lag.

Gas permeation

The permeability was measured with a classical θ apparatus.[14] The effective membrane area was 11.34 cm^2, and the permeate constant volume was 35.37 cm^3. The amount of gas transmitted at time t through the membrane was calculated from the permeate pressure (p_2 [cmHg/s]) readings in the low-pressure side of permeation cell. The permeability coefficients (P's) were obtained directly from the flow rate into the downstream volume when the steady state was reached:

$$P = \frac{Bl}{T_c p_1} \frac{dp_2}{dt} \tag{2}$$

where the cell constant $B = 11.53$ [cm^3(STP) K/(cm^2 cmHg)], p_1 is the pressure of high-pressure side (cmHg), and l is the membrane thickness (cm).

The membrane permselectivity or theoretical factors of separation (α) were calculated from the relation between the coefficient of pure gas permeation as

$$\alpha = \frac{P_i}{P_j} \tag{3}$$

where P_i and P_j are the permeabilities of i and j pure gases, respectively. θ measurements were made for the mixed matrix membranes as described previously for all of the gases, and it was calculated as follows:

$$\theta = \frac{l^2}{6D} \tag{4}$$

The apparent diffusion coefficient (D) was calculated from the θ data and the solubility coefficient (S) with the following equation according to Henry's law:

$$S = \frac{P}{D} \tag{5}$$

RESULTS AND DISCUSSION

OM analysis

Figure 2(a,b) shows images of the composite membranes prepared from PEI–AC. Samples containing 2 and 20 wt % AC were compared. Figure 2(a) shows that for PEI–2% AC, a good dispersion of inorganic filler in the polymer phase existed. Figure 2(b) shows the agglomerate formation in the polymer matrix when the AC concentration increased. The size of AC particles shown in Figure 2(a) was approximately 20 μm. This indicated that, when the AC content in the polymeric matrix was 2%, there were not nearly as much agglomerate formation and the particles showed good dispersion. However, when the AC content was 20%, the agglomerate sizes were between 200 and 400 μm, as shown in Figure 2(b). From the analysis obtained for PEI–10% AC (image not shown), an agglomerate size between 100 and 150 μm was determined.

Mechanical properties

The mechanical properties of the synthesized composite materials depended on several factors, such as the ratio of filler to polymer, the particle size, the degree of dispersion, and adhesion/contact in the interface. From the mechanical assays, typical tensile curves for each sample as a function of elongation were obtained. These results were used to determine the values of the mechanical parameters, that is, the elastic modulus, Young's modulus (E), rupture tension (σ), rupture elongation (ε), and toughness.

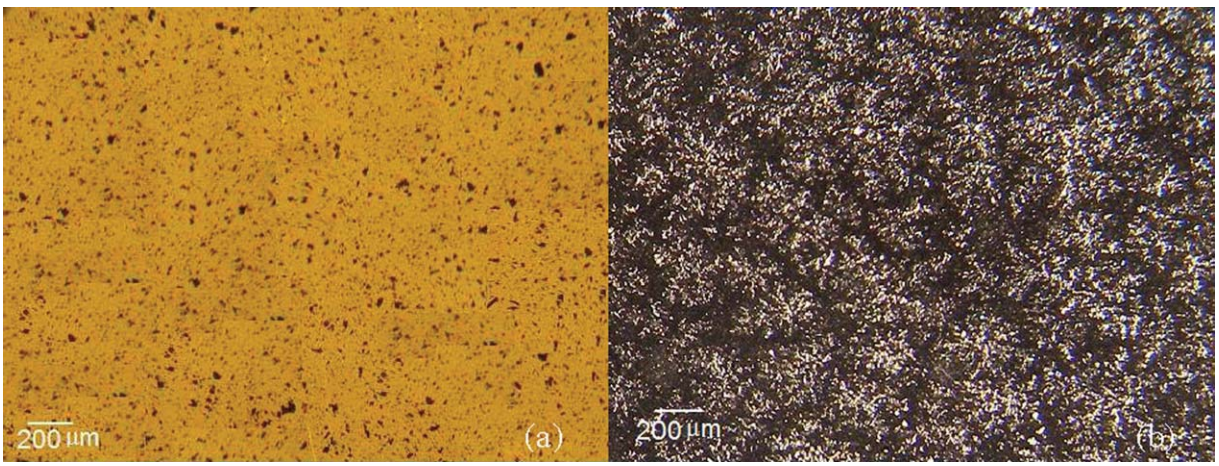

Figure 2 OM images of the (a) PEI–2% and (b) PEI–20% AC composite membranes. [Color figure can be viewed in the online issue, which is available at www.interscience.wiley.com.]

E was calculated from the slope of the stress–strain curve when a linear relationship between the stress and strain was observed. The tension at break and elongation at break were calculated as final points on the stress–strain curve, whereas the area under the stress–strain curve was used to characterize the value of the absorption energy before the fracture point, that is, the materials' toughness. The data obtained for each composite material of the mixed matrix are shown in Table I.

As shown in Table I, an increase in the resistance to tension of the PEI–2% AC membrane compared to that of the pure polymeric material (AC = 0%) was observed. With respect to the values of loaded AC between 2 and 20%, the rupture tension decreased noticeably. The *rupture tension* of a material is defined as the maximum stress that the material can sustain under uniaxial tensile loading. For microparticulate and nanoparticulate composites, this relies on the effectiveness of the stress transfer between the matrix and fillers. Factors such as particle size, particle/matrix interfacial strength, and particle loading significantly affect the composite rupture tension. According to Fu et al.,[21] the effect of the particle size on the tensile yield of a composite is that it increases as the particle size decreases. Smaller particles have a higher total surface area for a given particle loading. This indicates that the rupture tension increases with increasing surface area of the filled particles through a more efficient stress transfer mechanism. However, these researchers noted that, for particles larger than 80 nm, the tension at break from composites is reduced when the particle loading is increased. Our results indicate that there was a certain amount of loaded filler (AC = 2%) where the composite material exhibited the highest resistance to tension. When the inorganic filler load increased, the particles tended to form agglomerates. Those agglomerates behaved like bigger particles, and they were able to cause a decrease in the tensile strength of the composites PEI–10% AC and PEI–20% AC. In addition to particle size and loading, the filler/matrix interfacial adhesion also affected the rupture tension of the composite membranes. For poorly bonded particles, the stress transfer at the particle–polymer interface was inefficient. Thus, the particle could not carry any load, and the composite rupture tension decreased with increasing particle loading.[21]

TABLE I
Mechanical Properties of the Composite Membranes

Membrane	σ (MPa)	ε (%)	*E* (GPa)	Toughness (kJ/m^3)
PEI–0% AC	67.85	10.33	1.221	4620.3
PEI–2% AC	95.60	9.00	1.329	4223.9
PEI–10% AC	34.19	6.80	0.869	891.8
PEI–20% AC	14.91	6.60	0.614	532.5

These results are consistent with those reported by Kumar et al.[17] who obtained evidence that an increase in the content of carbon nanofibers (i.e., 2–3%) within a PEI matrix favors the formation of agglomerates or the cumulus of filler in a polymeric matrix. These agglomerates acted as sites of stress concentration when a load or tension was applied on the composite; this resulted in the rupture of the sample with low values of tension. The results obtained by these researchers suggest that there was a fraction of filler for each composite system above which the material resistance decreased when a certain tension was applied to it.

Table I shows the values of maximum elongation as a function of the carbon content and shows that, as the inorganic filler amount increased, there was a decrease in the polymer flexibility. This behavior

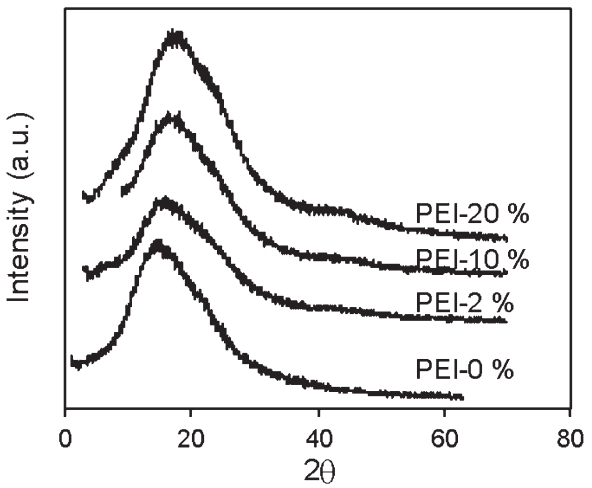

Figure 3 WAXD measurements of the composite membranes.

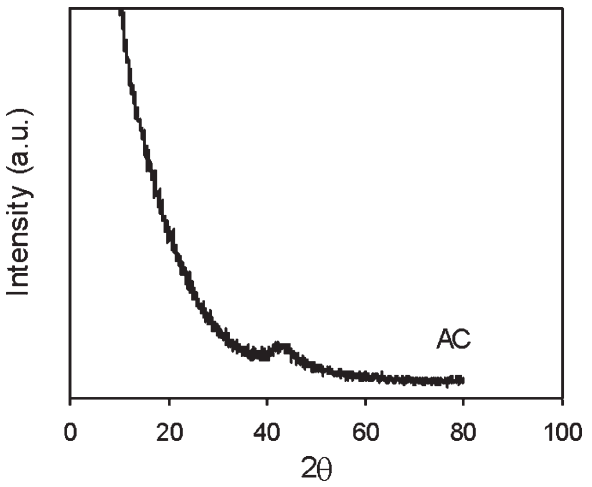

Figure 4 WAXD measurement of the AC Maxorb 3000.

was due to the carbon particles deposited on the PEI matrix, which acted as physical crosslinking points and restrained the movement of polymer chains; this caused a decrease in the polymer flexibility. Eisenberg et al.[22] proposed a model that suggests that the mobility of a polymer chain in the immediate vicinity of these multiplet clusters can become restricted relative to the rest of the chain in the bulk polymer.

The effect of AC addition on the elastic modulus of composites is also shown in Table I. The results show an increase in E with respect to pure PEI when the AC content was 2%. The addition of rigid particles to a polymer matrix can easily improve the modulus because the rigidity of inorganic fillers is generally much higher than that of organic polymers. The composite modulus consistently increased with increasing particle loading. This was in agreement with the tendency observed when the AC content increased from 0 to 2% for the PEI composite membranes. However, for high carbon loadings (10–20 wt %), a decrease in E was observed. The increment in agglomerate size produced a decrease in E. Similar results were reported by Fu et al.[21] for epoxy/glass composites with high glass bead loadings (30–46 vol %) and glass sizes between 2 and 30 μm.

The tenacity values reported in Table I indicate a decrease in the energy absorbed by the material during plastic deformation, before the rupture, as the AC content increased. At higher filler concentrations, toughening was not so efficient, probably because of the agglomeration of AC particles, which caused a weak interfacial adhesion. It is well known that strong interfacial adhesion leads to a high toughness in composite matrices. The results reported here reveal that, when the added particles formed agglomerates, the particle/matrix interfacial adhesion was weak, and a decrease in the fracture toughness was observed.

WAXD analysis

The WAXD technique constitutes a useful tool to study the arrangement of carbon at the molecular level.[23] Although the data of WAXD gives information about the center-to-center space of polymer chains and internal walls of carbon particles, there is no information that can be interpreted about the dimensions of micropores.[24] The WAXD data of the mixed matrix membranes and AC used as an inorganic filler are shown in Figures 3 and 4, respectively.

In the spectra of Figure 3, broad bands of different intensities in the range of 2θ between 15 and 25° are shown, whereas in Figure 4, a single band whose value of d (≈2.1 Å) corresponds to X-ray diffractograms of graphite carbon, specifically the plane (100) of graphite, is shown.[23,24] This signal started to appear within the range 30–50°. The intense bands in the range of 2θ between 15 and 25° were attributed to PEI matrix intercatenary distances. These broad bands presented a slight shift toward greater angles as the carbon content increased; that is, there was a structural arrangement of the polymer chains due to the presence of carbon.

In Table II, the d-spacing of the polymer (d_{pol}) is shown. It decreased as higher amounts of carbon were added. This indicated a decrease in the intercatenary distances. This behavior may have been due to a rigidification of the polymeric structure in the

TABLE II
Values of d-Spacing for the Composite Materials and AC

Membrane	d_{pol}	d_{AC}
PEI–0% AC	5.318	
PEI–2% AC	5.235	2.134
PEI–10% AC	5.112	2.134
PEI–20% AC	4.806	2.134

d_{pol} = d-spacing of the polymer; d_{AC} = d-spacing of the activated carbon.

TABLE III
Gas Permeability and Gas α Values

Membrane	P_{H_2} (B)	P_{N_2} (B)	P_{O_2} (B)	P_{CH_4} (B)	P_{CO_2} (B)	$\alpha_{H_2CH_4}$	$\alpha_{H_2CO_2}$	α_{H_2/O_2}	α_{H_2/N_2}	α_{CO_2/CH_4}	α_{O_2/N_2}
PEI–0% AC	6.904	0.051	0.373	0.029	1.561	238.07	4.42	18.51	135.37	53.83	7.31
PEI–2% AC	11.060	0.111	0.838	0.044	2.061	251.36	5.37	13.20	99.64	46.84	7.55
PEI–10% AC	13.510	0.132	1.073	0.050	2.087	270.20	6.47	12.59	102.35	41.74	8.13

$T_c = 30°C$ and $p_1 = 5$ atm. B = 1 Barrer = 10^{-10} cm^3(STP) cm/cm^2 cmHg s.

immediate vicinity of the filler particles. This rigidification process was also found by Vu et al.,[18] who worked with Matrimid 5218/CMS mixed matrix membranes for O_2/N_2 separation. Those authors observed that the filler CMS particles were surrounded by an interfacial layer of more rigid matrix material and reported an elevation in the glass-transition temperature as a result. A similar effect was reported by Mahajan and Koros[25,26] in mixed matrix membranes of poly(vinyl acetate)/zeolite 4A and BAPB–BPADA/zeolite 4A for O_2/N_2 separation. The change in rigidity found was in agreement with the decrease in the flexibility of composite materials as the filler content increased reported in the Mechanical Properties section.

Gas permeation measurements

The permeability was measured in all of the assayed gases and membranes at $T = 30°C$ and $p_1 = 5$ atm. Because of the high fragility of the PEI–20% AC membrane, we could not subjected it to gas permeability tests. The individual gases were measured in the following order: H_2, N_2, O_2, CH_4, and CO_2 to avoid the effects of plasticization. The coefficients of permeability determined for the pure PEI membrane and those loaded with 2 and 10% AC are summarized in Table III, and they were obtained by the averaging of the values attained from three samples of each membrane. The results show an increase in the permeability of all of the gases with increasing AC amount. The increment in the gas permeability of the composite membranes over the pure PEI matrix were attributed to the low gas flux resistance of the carbon porous particles and the poor interfacial contact between the inorganic filler and the polymeric matrix, as mentioned in the Mechanical Properties section. These particles had an ε value of 0.87 and a relatively high pore size (d = 21.7 Å) compared to the gas kinetic diameter.

The permeation of a polymeric dense membrane by a penetrant gas is generally considered to be a solution–diffusion process.[27] According with this mechanism, gas permeation is a complex process that involves first the sorption of the penetrant in the polymeric material, followed by the diffusion of a gas molecule across the membrane matrix because of a concentration gradient. The kinetic diameter, which corresponds more closely to the minimum diameter of the molecule, has a strong effect on the penetrant mobility. It is evident that the smaller the penetrant kinetic diameter is, the higher the penetrant mobility will be through the polymer gaps to reach a new site. It is clear from Table III and the data of kinetic diameters (σ_{kH_2} = 2.89 Å, σ_{kCO_2} = 3.36 Å, σ_{kO_2} = 3.46 Å, σ_{kN_2} = 3.64 Å, and σ_{kCH_4} = 3.80 Å) that there was a good correlation between the permeation coefficients ($P_{H_2} > P_{CO_2} > P_{O_2} > P_{N_2} > P_{CH_4}$) and their kinetic diameters ($\sigma_{kH_2} < \sigma_{kCO_2} < \sigma_{kO_2} < \sigma_{kN_2} < \sigma_{kCH_4}$). Figure 5 shows the linear relationship between the permeation coefficients and the kinetic diameters of the gases for PEI–2% AC. The same behavior was observed in PEI with 0 and 10% AC.

To analyze the composite material permselectivity, the H_2/CH_4, H_2/CO_2, H_2/N_2, H_2/O_2, O_2/N_2, and CO_2/CH_4 systems were chosen because of the importance of their commercial use and purification. Table III shows the relative effects of the amount of AC loaded on the ideal separation factor for the selected systems through the PEI–AC composite membranes, as evaluated from eq. (3). As shown in the table, the PEI–AC membranes showed interesting separation factors for all of the systems analyzed, particularly the H_2/CH_4, H_2/CO_2, and O_2/N_2 systems, where there was a simultaneous increase of gas permeability and selectivity with increasing

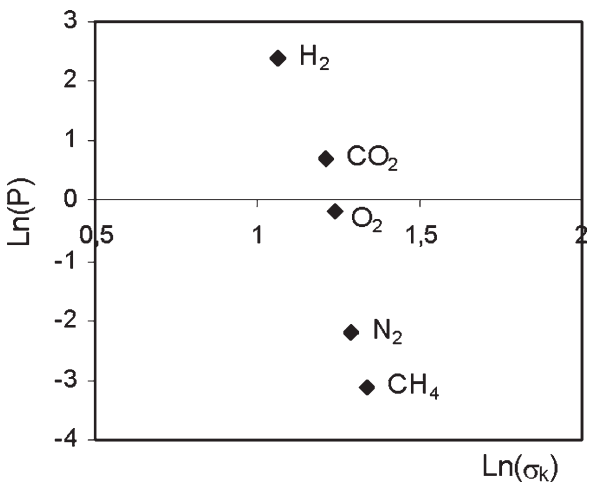

Figure 5 Correlation of the permeation coefficients versus penetrant kinetic diameters in the PEI–2% AC membrane.

TABLE IV
Apparent Diffusivity and Solubility Coefficients as a Function of the AC Content

Membrane	D_{N_2}	D_{O_2}	D_{CH_4}	D_{CO_2}	S_{N_2}	S_{O_2}	S_{CH_4}	S_{CO_2}
PEI–0% AC	0.024	0.037	0.009	0.017	0.022	0.101	0.032	0.943
PEI–2% AC	0.021	0.039	0.019	0.013	0.053	0.211	0.023	1.651
PEI–10% AC	0.026	0.035	0.010	0.011	0.050	0.310	0.050	1.898

$T_c = 30°C$, $p_1 = 5$ atm, $D = 10^{-6}$ cm^2/s, $S = 10^{-2}$ cm^3(STP)/cm^3 cmHg.

percentage of carbon loaded on the composite membranes. An increase in gas permeability usually suggests the presence of interfacial defects that increase gas permeability but with a loss in the selectivity. However, in this case, the ideal selectivities of the H_2/CH_4, H_2/CO_2, and O_2/N_2 systems increased from 238.07, 4.42, and 7.31 to 270.20, 6.47, and 8.13 for pure and 10% AC loaded PEI, respectively. To explain this behavior, in Table IV, the gas diffusion and solubility coefficients are shown. As the filler content increased, the diffusion coefficients decreased for O_2, CO_2, and CH_4. This behavior was due to the polymer phase rigidification, even when the interfacial defects were present in the composite membrane. However, the apparent solubility for these gases increased as the carbon content increased. This behavior indicated that there was a preferential sorption of those gases in the carbon particles or in the interface particle/polymer. The hydrogen θ values were too short to be measured accurately. N_2, an inert gas, did not show a marked effect of sorption as the carbon content increased, whereas its diffusion was less affected by the polymer phase rigidification. As an overall result, the polymer phase rigidification favored the size exclusion selectivity, and it decreased the gas diffusion coefficients, whereas a preferential gas sorption for certain gases constituted a weight factor, which increased the permeation coefficients of these gases and caused the gas selectivity observed for this type of composite membranes.[28,29]

A comparison of the O_2/N_2 separation performance for PEI–10% AC membrane with the Robeson's trade-off lines (prior and present upper bound[30–32]) is shown in Figure 6, where the composite PEI selectivity of other authors is included. Koros et al.[18] reported O_2/N_2 selectivities of 7.3 and 8 at $T = 35°C$ and $p_1 = 3.4$ atm for both pure and 35% CMS loaded PEI, respectively. On the other hand, Takahashi and Paul[33] investigated the relation between the extent of voids formed in nanocomposite of PEI and three kinds of hydrophobically treated fumed silica and the permeation properties. These researchers found O_2/N_2 selectivities of 6.75, 6.44, 5.78, and 4.79 for all-pure, TS610-10 methyl-treated, TS530-10 trimethylsilyl-treated, and TS720-10 polydimethylsiloxane (PDMS)-treated PEIs (at $T = 35°C$ and $p_1 = 3$ atm). The ideal O_2/N_2 selectivities for the PEI–AC composites were among the highest reported for PEI-based composite membranes.

CONCLUSIONS

In this study, acknowledged characterization techniques were used to study the effects of particle size, particle/polymer adhesion, and particle agglomeration on the structural and permselective properties of PEI–AC composites membranes. OM images evidenced agglomerate formation as the inorganic filler content increased. The tension at break depended on the carbon particle surface area. This contact area allowed effective stress transfer between the filler and matrix. The elongation at break was affected by the restriction of movement of the polymer chains because the AC agglomerates acted as sites of stress concentration within the polymer matrix. The toughness was controlled by adhesion between the carbon particles and polymer. On the other hand, the particle size affected the modulus because an increment in the agglomerates size produced a decrease in the E value. The study of WAXD showed a clear influence of carbon on the structural arrangement of the polymeric matrix, which decreased the intercatenary distances. The decrease in d-spacing values was in

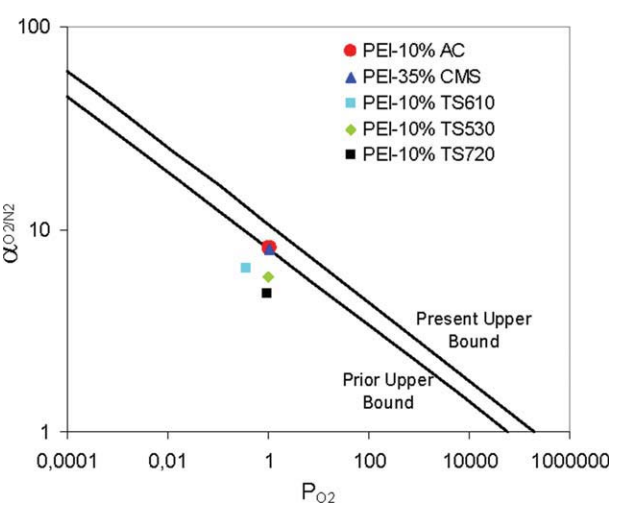

Figure 6 O_2/N_2 selectivity for PEI composites: PEI–10%AC (this study), PEI–35% CMS,[18] PEI–10% TS610, PEI–10% TS530, and PEI–10% TS720.[32] [Color figure can be viewed in the online issue, which is available at www.interscience.wiley.com.]

agreement with the decrease in the composites elongation and the polymer matrix rigidity as the carbon content increased.

The permselectivity characteristics of H_2/CH_4, H_2/CO_2, and O_2/N_2 pairs for pure and loaded PEI were analyzed. Poor particle/polymer interfacial adhesion caused an increase in all of gas permeabilities as the inorganic filler loading increased. Interestingly, the selective diffusion and sorption of certain gases resulted in increments in the H_2/CH_4, H_2/CO_2 and O_2/N_2 selectivities. Diffusion selectivities were associated with polymeric matrix rigidification, and solubility selectivities were associated with a preferential sorption of gases in the inorganic AC filler. The ideal O_2/N_2 selectivities for PEI–AC were among the highest values reported for PEI-based composite membranes.

References

1. Paul, D. R.; Kemp D. R. J Polym Sci Part C: Polym Symp 1973, 41, 79.
2. Kulprathipanja, S.; Neuzil, R. W.; Li N. N. (to Allied-Signal, Inc.). U.S. Pat. 4,740,219 (1988).
3. te Hennepe, H. J. C. Ph.D. thesis, University of Twente, 1988.
4. Gurkan, T.; Bac, N.; Kiran, G.; Gur, T. Proceedings of the 6th International Symposium on Synthetic Membranes in Science and Industry, European Membrane Society, Tübingen, Germany, 1989.
5. Hillock, A. M. W.; Koros W. J. Macromolecules 2007, 40, 583.
6. Kita, H.; Inada, T.; Tanaka, K.; Okamoto, K. J Membr Sci 1994, 87, 139.
7. Liu, Y.; Pan, C.; Ding, M. X.; Xu, J. P. J Appl Polym Sci 1999, 73, 521.
8. Bos, A.; Punt, I. G. M.; Wessling, M.; Strathmann, H. Sep Purif Tech 1998, 14, 27.
9. Krol, J. J.; Boerrigter, M.; Koops, G. H. J Membr Sci 2001, 184, 275.
10. Wind, J. D.; Staudt-Bickel, C.; Paul, D. R.; Koros, W. J. Macromolecules 2003, 36, 1882.
11. Wind, J. D.; Sirard, S. M.; Paul, D. R.; Green, P. F.; Johnston, K. P.; Koros, W. J. Macromolecules 2003, 36; 6433.
12. Shao, L.; Chunga, T.-S.; Goh, S. H.; Pramoda, K. P. J Membr Sci 2004, 238, 153.
13. Zhou, Y.; Pervin, F.; Rangari, V. K.; Jeelani, S. Mater Sci Eng A 2006, 426, 221.
14. Marchese, J.; Garis, E.; Anson, M.; Ochoa, N. A.; Pagliero, C. J Membr Sci 2004, 243, 19.
15. Koros, W. J.; Mahajan, R. J Membr Sci 2000, 175, 181.
16. Duval, J. M.; Kemperman, A. J. B.; Folkers, B.; Mulder, M. H. V.; Desgrandchamps, G.; Smolders, C. A. J Appl Polym Sci 1994, 54, 409.
17. Kumar, S.; Rath, T.; Mahaling, R. N.; Reddy, C. S.; Das, C. K.; Pandey, K. N.; Srivastava, R. B.; Yadaw, S. B. Mater Sci Eng B 2007, 141, 61.
18. Vu, D. Q.; Koros, W. J.; Miller, S. J. J Membr Sci 2003, 211, 311.
19. Marchese, J.; Anson, M.; Ochoa, N. A., Prádanos, P.; Palacio, L.; Hernández, A. Chem Eng Sci 2006, 61, 5448.
20. Vankelecom, I. F. J.; Merckx, E.; Luts, M.; Uytterhoeven, J. B. J Phys Chem 1995, 99, 13187.
21. Fu, S.-Y; Feng, X.-Q.; Lauke, B.; Mai, Y.-W. Compos B 2008, 39, 933.
22. Eisenberg, A.; Hird, B.; Moore, R. B. Macromolecules 1990, 23, 4098.
23. Xiao, Y.; Chung, T.-S.; Chng, M. L.; Tamai, S.; Yamaguchi, A. J Phys Chem B 2005, 109, 18741.
24. Steel, K. M.; Koros, W. J. Carbon 2003, 41, 253.
25. Mahajan, R.; Koros, W. J. Ind Eng Chem Res 2000, 39, 2692.
26. Mahajan, R.; Koros, W. J. Poly Eng Sci 2004, 42, 1420.
27. Koros, W. J.; Fleming, G. K. J Membr Sci 1993, 83, 1.
28. Zhang, Y.; Musselman, I. H.; Ferraris, J. P.; Balkus, K. J., Jr. J Membr Sci 2008, 313, 170.
29. Zhang, Y.; Musselman, I. H.; Ferraris, J. P.; Balkus, K. J., Jr. Ind Eng Chem Res 2008, 47, 2794.
30. Robeson, L. M. J Membr Sci 1991, 62, 165.
31. Robeson, L. M.; Burgoyne, W. F.; Langsam, M.; Savoca, A. C.; Tien, C. F. Polymer 1994, 35, 4970.
32. Robeson, L. M. J Membr Sci 2008, 320, 390.
33. Takahashi, S.; Paul, D. R. Polymer 2006, 47, 7519.